CONSTRUCTION
E-ISSN: 2785-8731
VOLUME 5, ISSUE 2, 2025, 287 - 295
DOI: https://doi.org/10.15282/construction.v5i2.12333

RESEARCH ARTICLE

Investigation of Energy Dissipation for a Submerged Breakwater Using Computational Fluid Dynamic Model Flow-3D

Izzah Khairil[1], Saerahany Ibrahim[1]*, Izihan Ibrahim[1], Ayishah Thaminah Hikmatullah Sahib[2], Zahir Ramli[2], Amarif Abimunya[3]

[1]Department of Civil Engineering, International Islamic University, Malaysia
[2]Department of Marine Science, International Islamic University, Malaysia
[3]Marine Research Laboratory (MEAL), Universitas Padjadjaran, Indonesia

ABSTRACT - The dynamic interaction between waves and coastal structures is an ongoing challenge, and the performance of submerged breakwaters is essential for coastal protection. As physical modeling is costly and complex, this study uses Computational Fluid Dynamics (CFD) to numerically investigate wave behaviour and energy dissipation over a submerged horizontal breakwater with a 0.5-meter head above its crest. The methodology employs the FLOW-3D software, solving the Reynolds-Averaged Navier-Stokes (RANS) equations coupled with the Volume of Fluid (VOF) method for free-surface tracking. The main findings confirm the model's capability to accurately simulate wave run-up and energy dissipation. This demonstrates the utility of FLOW-3D as a dependable, cost-effective alternative to physical experimentation for optimizing submerged breakwater designs and enhancing coastal stability.

ARTICLE HISTORY
Received : 24 April 2025
Revised : 27 November 2025
Accepted : 19 December 2025
Published : 29 December 2025

KEYWORDS
Submerged breakwater
Flow-3D
Energy dissipation
Computational fluid dynamics

1. INTRODUCTION

Submerged breakwaters are an efficient way to prevent coastal erosion, keeping the basin calm, reducing siltation at the harbor entrances and along the approach channel, protecting marine habitats, while also taking account the sustainability factor. Breakwaters that are submerged allow for the exchange of water masses between the offshore and onshore region, reducing beach pollution. The width and depth of the submerged breakwater's submergence, the distance of the structure from the shore, its hydrodynamic properties, the wave climate, and the wave attack angle all play a role in how much coastal protection it offers [1]. Submerged breakwaters (Figure 1) are widely used in coastal engineering to reduce wave energy and protect shorelines without obstructing ocean views. Their effectiveness in dissipating wave energy depends on factors such as geometry, porosity, submergence depth, and arrangement. Recent research combines experimental, numerical, and field studies to optimize their design for maximum energy dissipation.

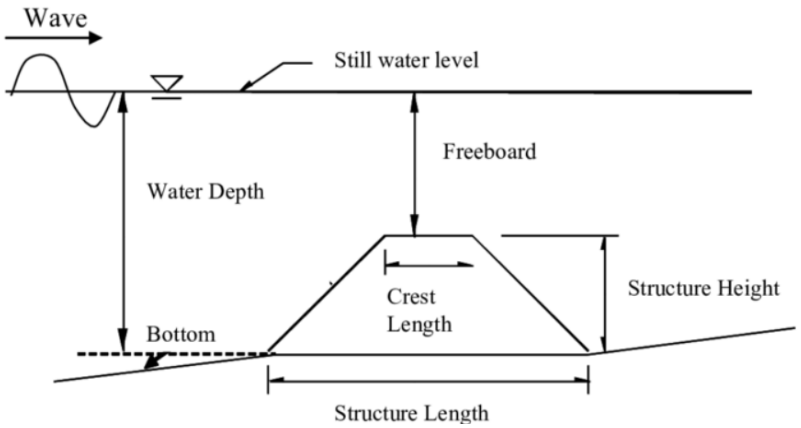

Figure. 1 Schematic diagram of a submerged breakwater [2]

Depth-limited wave breaking over the crest and turbulence generated by flow through or around the structure are primary sources of energy loss [3]. Eddies and vortices, especially behind and above the breakwater, contribute significantly to energy dissipation [4]. Permeable breakwaters enhance dissipation by increasing turbulence within the structure, with optimal porosity typically between 0.2 and 0.3 [5]. Double or stepped breakwaters dissipate more energy than single or smooth ones, with energy loss concentrated near the first bar during Bragg resonance [6]. Increased porosity and width generally improve dissipation, but excessive porosity can reduce effectiveness [5]. Greater submergence (higher h/d ratio) and wider breakwaters increase energy dissipation, with coefficients (Kd) reaching up to 0.95 for highly submerged, solid breakwaters [6]. Perforated, gyroid, and multi-layered designs show promise for broad-spectrum wave attenuation [7]. Submerged breakwaters effectively dissipate wave energy through breaking, turbulence, and vortex

***CORRESPONDING AUTHOR | Saerahny Ibrahim** | ✉ saerahany@iium.edu.my

formation. Their performance is maximized by optimizing shape, porosity, width, and submergence depth. Recent innovations in design and modeling continue to improve their efficiency, making them vital tools for sustainable coastal protection.

A large portion of research on using computational fluid dynamics (CFD) for breakwater modeling has been carried out using various simulation programs. The results from these studies, which employed FLOW-3D to simulate diverse hydraulic structures, showed a reasonable level of agreement with both experimental data and conventional design standards. Nonetheless, there are numerous other software packages that are employed to model flow through breakwaters and investigate their hydraulic behavior. This includes information on the effective use of CFD and Fluent software, as well as comparisons of CFD and Fluent. Previous research on hydraulic issues has shown that both FLOW-3D and Fluent are effective tools for tackling advanced fluid-solid interaction problems and can provide significant results. The investigation of energy dissipation in breakwaters through CFD models reveals consistent findings across various studies. An investigation demonstrated that transmission coefficients increase with incident wave height and that energy dissipation is highest at zero submerged depth for certain breakwater types, such as sloped steps models [8]. Another recent experiment was conducted that proved double-submerged semicircular breakwaters dissipation wave energy is able to be simulated using one of CFD turbulence model which is similarly to the study from Cheng et al. in 2022 that found the turbulence and mixing within porous composite breakwaters that was successfully proved using three-dimensional Reynolds-averaged Navier-Stokes equation with the closure of renormalization group k−ε turbulence model and volume of fluid method [9][10]. Across these studies, CFD simulations aligned well with experimental data, validating their effectiveness in predicting wave-structure interactions and energy dissipation mechanisms. In 1994, Grilli and colleagues conducted laboratory experiments using a nonlinear potential model to study the breaking of individual waves on breakwaters. They observed that waves could collapse over the crest, break forward or backward over submerged breakwaters, or do all three, depending on the height of the incoming wave. The experiments also yielded information on wave transmission and reflection coefficients. The results showed that transmission coefficients increased to a range of 55% to 90% for submerged breakwaters. The nonlinear potential model was able to accurately predict the limit of collapse for submerged breakwaters, especially for lower wave heights. Overall, the model calculations were consistent with the laboratory observations [11].

With the aid of computational fluid dynamics (CFD), FLOW-3D a prediction regarding the hydrodynamic characteristics of a submerged breakwater is presented in this paper. The CFD used for this study is FLOW-3D, several parameters have been simulated to determine how the coefficient of transmission and energy dissipation resulted from the presence of submerged breakwater. The kinetic energy per unit volume of fluid is linked to dynamic pressure, which shows a direct correlation with resistance [11]. Kawasaki conducted a study on the deformation process of breaking and post-breaking waves around a submerged breakwater in a two-dimensional wave field in the vertical plane [12]. The model used a non-reflective wave generator combined with the VOF approach and dissipation zone with open boundary conditions. The model not only looked at wave breaking over a submerged breakwater but also at the distortion of waves after they broke. Experiments were conducted to verify the reliability of the model, looking at the height of incident waves and the frequency of wave amplitude. The results showed that a wave-breaking-induced circulating flow occurs on the onshore side of the submerged breakwater, both before and after wave breaking. The proposed numerical wave model accurately simulated wave deformation by comparing its results with experimental data [12]. Despite general agreement on the key influences of wave height, submerged depth, and breakwater design on energy dissipation, some variances exist due to modeling approaches and assumptions. Different numerical methods—such as boundary integral element methods and volume of fluid techniques which affect the detailed quantification of energy loss and computational efficiency. Overall, these studies collectively advance the understanding of breakwater energy dissipation, confirming the robustness of CFD as a tool while highlighting the need for harmonized modeling standards.

In this paper, the main objective of the research is to numerically investigate wave behavior and energy dissipation over a submerged horizontal breakwater using CFD, specifically demonstrating the capability of the FLOW-3D software as a reliable alternative to physical modeling.

1.1 Turbulence Model Selection

The RNG (Renormalization Group) k-ε turbulence model is an advanced two-equation model derived from statistical methods to improve predictions of turbulent flows, especially those involving strong separation, swirling, and rapid strain. It modifies the standard k-ε model by introducing additional terms in the dissipation rate (ε) equation, allowing for better treatment of turbulence in complex, high-Reynolds-number, and near-wall flows which in this case is the flow's interaction with the breakwater [13][14].

Like the standard k-ε model, the RNG k-ε model solves two transport equations, one for turbulent kinetic energy (k) and one for its dissipation rate (ε). The RNG approach analytically derives the turbulent Prandtl numbers and introduces a correction term in the ε equation to account for the effects of mean strain and streamline curvature[13][14]. The RNG model explicitly incorporates the influence of swirling and rotating flows, which are common in vortex shedding and flow separation scenarios [13][14][15]. The model is more accurate for low-Reynolds-number effects near solid boundaries, improving predictions in boundary layers and regions of flow detachment [14][16]. The RNG k-ε model is less dissipative than the standard k-ε, leading to more accurate simulation of recirculatory flows and separation zones, such as those found near breakwater crests or backward-facing steps [17][13]. It better captures moderate-scale vortices

and turbulent kinetic energy fields, closely matching experimental data for vortex shedding and mean velocity near solid boundaries [18]. The RNG k-ε model can more accurately simulate the formation and evolution of vortices near the free surface, where breaking and strong turbulence occurs, due to its improved handling of strain and curvature [19][16]. It offers a good balance between computational cost and accuracy, making it suitable for large-scale engineering simulations where full Reynolds Stress Models (RSM) or LES would be too expensive [14][15].

The RNG k-ε model is selected as compared to the standard k-ε for simulating flow separation and vortex shedding near solid boundaries and free surfaces due to its enhanced treatment of turbulence anisotropy, swirl, and near-wall effects, providing more accurate and reliable results in complex flow scenarios [17][13][18].

2. METHODS AND MATERIALS

The current research employs the FLOW-3D computational fluid dynamics model, which can consider a variety of fluid boundary conditions and solve for the interface between fluids and between fluids and air. This model is utilized in a range of applications within hydraulic engineering and coastal environments, including the study of fluid flow and erosion around hydraulic structures, as well as wave transmission in coastal areas. The FLOW-3D model solves the three-dimensional Navier-Stokes equations and continuity equation at the same time to describe fluid behavior in accordance with the general Navier-Stokes equation [20].

$$\frac{\partial u_i}{\partial x_i} = 0 \tag{1}$$

$$\frac{\partial u_i}{\partial t} + u_j \frac{\partial u_j}{\partial x_j} = \frac{1}{\rho}\frac{\partial \rho}{\partial x_i} + v\frac{\partial^2 u_i}{\partial x_j \partial x_j} + g_i \tag{2}$$

The Fractional Area-Volume Obstacle Representation (FAVOR) method is used to simulate rigid boundaries. This technique calculates the area occupied by a cell by determining the open volume and area of the cell. The resulting area/volume ratios are then utilized in the Navier-Stokes equations as factors for estimating the dynamic properties of the fluid [21]. The RNG turbulence model were combined and integrated into simulations on a numerical flume with a flat bottom. The three-dimensional space was divided into two mesh blocks - a larger one in front of the breakwater and a finer one in the more complex hydrodynamic area around the breakwater. This was done to ensure that enough computing nodes were available to accurately evaluate the filtration motion of the flow.

The developed model was validated upon the completion of the simulations to which it was obtained by the wave transmission equation in comparison to the values extracted from FLOW-3D. The comparison yielded a strong correlation coefficient (R^2) of 0.73, confirming the model's reliability according to the standard extracted from a study conducted on evaluation of coastal hydrodynamic performance using statistical analysis at the Kelantan coast, Malaysia [22]. These results demonstrate that the RNG turbulence model is suitable for its intended purpose in investigating the dissipation of a submerged breakwater using FLOW-3D.

2.1 Model Set-up

The overall design of the model closely resembled that of all the controlled breaking wave simulations. The fluid parameters for each simulation were set to be identical to those of water at 20 degrees Celsius. The boundaries of the free surface in FLOW-3D are defined by the top boundary, which is typically defined as a free surface. This means that the fluid is free to move in any direction at the top boundary. In this scenario, the top boundary was defined as atmospheric pressure, the bottom boundary was defined as a wall, and the bottom boundary of the model's geometry was moved to just below the input form while the crest of the breakwater was moved to 0.5 meters just below the initial water level. Although there were numerous physical options to choose from, only two were necessary for accurate simulations of the desired data in this study. The gravity option was activated when the acceleration of gravity in the vertical, or z-direction, reached -9.81 meters per second. When applying Newtonian viscosity and selecting an appropriate turbulence model for the flow, the option to activate viscosity and turbulence was also turned on simultaneously as well as the shallow water option. Once the FLOW 3D model was fully constructed and the two-equation (k-w) model was selected, only one turbulence model was applied.

The process of preparing the numerical model's geometry was different from other breaking wave simulations previously done in FLOW-3D. The geometry used in the simulations were modelled in AUTOCAD 3D modelling. The typical value of concrete roughness for the flume geometry was set to be 0.035 that complies with the Manning's classification of coastal structures. The breakwater was determined to have a trapezoidal shape almost in conjunction with NAHRIM's breakwater experiment called the WABCORE. The initial study was supposed to see the efficiency of breakwater using the exact model of WABCORE but due to simplification and time constrain, the breakwater remained conventional. The size of the breakwater for this report has a length of 12 meters, the height of 0.75 meters and the width of 3 meters.

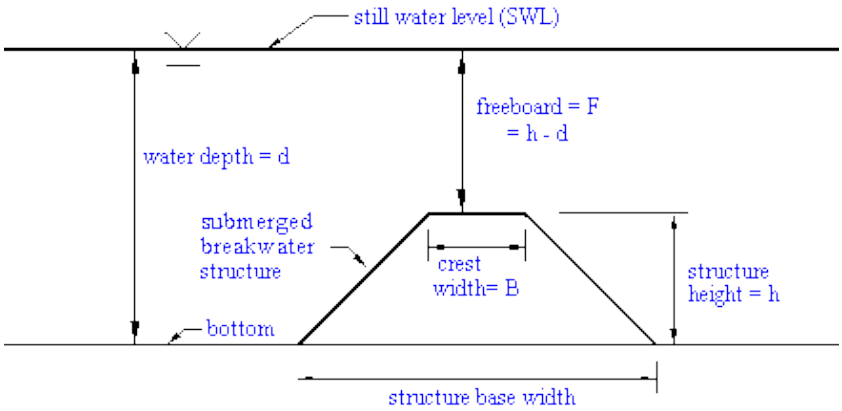

Figure. 2 Definition sketches for a submerged breakwater

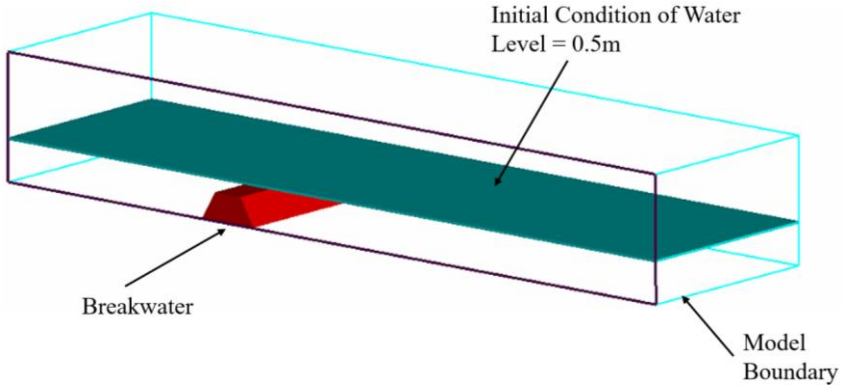

Figure. 3 Model of horizontal breakwater in FLOW-3D

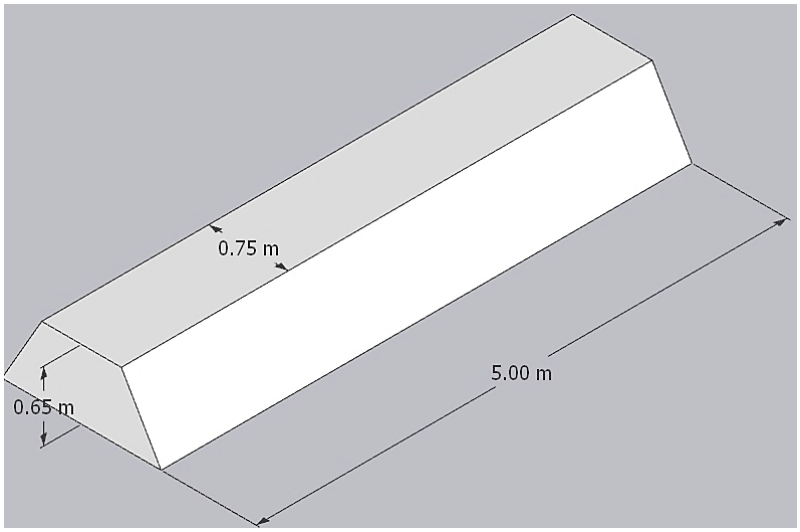

Figure. 4 Solid model of horizontal breakwater

To set up the simulation, the parameters of the environment surrounding the breakwater must be determined. With few features on the FLOW-3D that allow customization of wave design, few parameters have been selected. For this research, a singular solitary wave was designed which is also known as a soliton, a type of wave that maintains its shape and speed as it propagates through a medium. It is often described as a "hump" or "bump" that travels through a fluid without breaking or dispersing [23]. Other than that, ocean waves are classified as solitary waves and are suitable for this experiment because the breakwater used is submerged under shallow water.

The calculation of shallow water is derived from the linear wave theory which is the theory that would be opted for this report and is a good approximation under the Navier-Stokes numerical model. “Extensions of the present analysis and synthesis approach to Navier-Stokes equations appear to be straightforward if one deals with a set of consistently linearized operators” [24]. The solitary wave option under FLOW-3D allows the user to edit wave attributes from wave

height, mean fluid depth and velocities. To scrutinize the features of the wave, the fluid's initial condition must be determined and for this experiment, the undisturbed water depth is equal to the mean fluid depth with the value of 1.15 meters. The celerity can also be determined so the speed of 5 m/s was chosen to stay within the relevance of shallow water as well as 10s for the period set on this model. To validate this experiment being under the category of shallow water, a calculation to find the ratio of depth to wavelength is done to ensure that the value is less than 0.05.

Finding wavelength, λ.

$$L = \frac{gT^2}{2\pi}\tanh(\frac{2\pi d}{L}) \tag{4}$$

$$L = \frac{(9.81)(10)^2}{2\pi}\tanh[\frac{2\pi(2.5)}{L}] \tag{5}$$

$$L = 92.4m \tag{6}$$

Relative depth;

$$\frac{d}{L} = \frac{2.5}{92.4} \tag{7}$$

$$\frac{d}{L} = 0.012 < \frac{1}{20} \tag{8}$$

∴ Shallow water

Table 2. Wave classification by relative depth for linear wave

Classification	d/L	kd	tanh (kd)
Deep Water	1/2 to ∞	Π to ∞	≈ 1
Transitional	1/20 to 1/2	Π/10 to Π	tanh (kd)
Shallow Water	0 to 1/20	0 to Π/10	≈ kd

The initial conditions for a solitary wave include its height, width, and speed. The wave height represents the maximum displacement of the water surface from its equilibrium position, while the width is the distance between the crest and trough. The velocity indicates the speed at which the wave travels. Key parameters include the wavelength L, which is the horizontal distance between successive wave crests; gravitational acceleration $g = 9.81\ \text{m/s}^2$; wave period T, the time for one wavelength to pass a point (here 10 seconds); and water depth d (here 2.5 meters). The first calculation applies the linear wave dispersion relation to find the wavelength L, resulting in 92.4 meters. Next, the relative depth d/L is calculated as the ratio of water depth to wavelength, $2.5/92.4 = 0.027$. This ratio is crucial for wave classification. Since 0.027 is less than 0.05 (or 1/20), the wave is classified as a shallow water wave, indicating that the wave motion is influenced by the seabed throughout its entire depth. This classification can ensure practicality in analyzing the phenomenon of wave energy and velocity.

2.2 Boundary Conditions

To accurately simulate the propagation of the solitary wave and isolate the energy dissipation caused by the breakwater, the numerical flume was equipped with specific boundary conditions. The inflow boundary, where the wave is generated, was defined as a wave velocity to ensure the non-reflective generation of the solitary wave, following the methodology of Wang et al., [5]. Conversely, the outflow boundary at the end of the set up was set to outflow to prevent wave reflection back into the domain, ensuring that only the energy transmitted through the breakwater was measured.

3. RESULTS AND DISCUSSION

Most simulations used default settings, including default time step parameters. However, in some cases, shorter ending times were necessary to find a convergent solution. Simulations were typically completed using the default explicit solver settings, but some simulations used the implicit solution method.

3.1 Wave Transformation and Turbulence Dissipation

According to images above from the post-process of FLOW-3D, it is seen that as the wave passes the submerged breakwater, a significant reduction of height is displayed. Before the wave interacts with the submerged structure, the turbulent energy contours (Figure. 4) confirm a near-laminar flow state in the incident wave field, with maximum turbulent kinetic energy values remaining below 0.0002. As the wave begins to climb the structure's upward slope at approximately x= 2.5m the phenomenon of wave shoaling initiates, resulting in a measurable increase in wave height from the undisturbed depth and a subsequent steepening of the wave face.

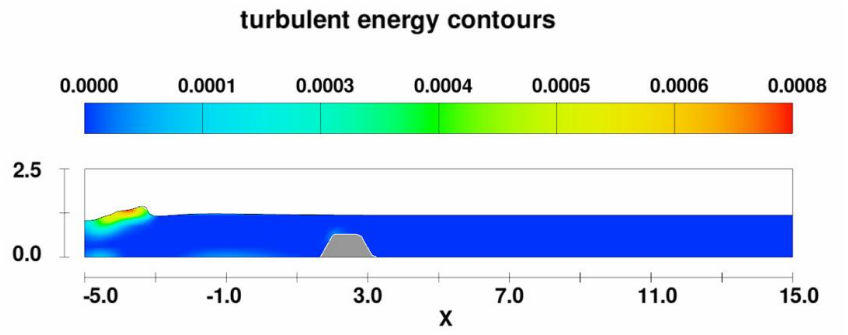

Figure. 4 2D Postprocess waves before breakwater

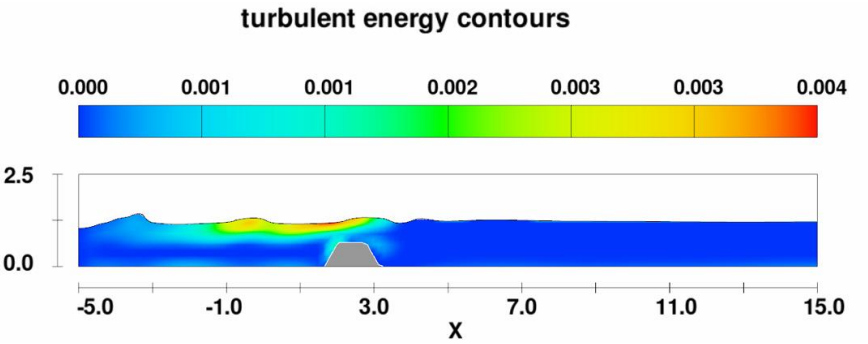

Figure. 5 2D Postprocess waves on breakwater

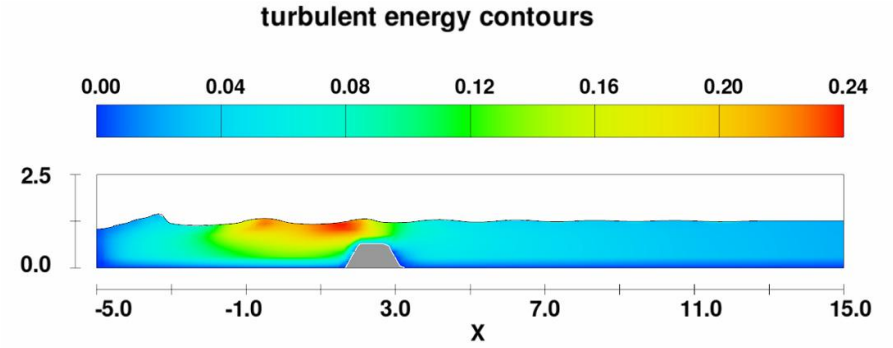

Figure. 6 2D Postprocess waves after breakwater

As the wave passes over the structure, the primary energy dissipation mechanism is captured in Figure 5, illustrating the process of wave-breaking and subsequent collapse of the crest over the breakwater. Interpretation of the turbulent energy contours reveals a distinct peak in the turbulent kinetic energy (TKE) magnitude, reaching approximately 0.004 directly above the structure's crest which is at the approximate x-coordinate of x = 3.0m. This high concentration of TKE, indicated by the intense yellow and red coloring, represents the conversion of coherent wave energy into internal turbulent motion, confirming the crest collapse as the single most significant source of energy loss in this submerged configuration. Following the primary breaking event, the turbulent flow continues to dissipate energy on the lee side (downstream) of the structure, as depicted in Figure 6. The turbulent wake, which resembles a spilling breaker, extends from the crest at x=3.5m to approximately x=0.10m. This sustained turbulence, characterized by elevated TKE values of up to approximately 0.24, is maintained by the sustained shear stress and intense mixing as the wave attempts to reform, representing a crucial component of the total energy loss.

From the graph above, it is seen a sudden drop of wave amplitude after it has passed the breakwater at x = 0. After the wave has passed the breakwater, it is seen a gentle descent of the wave height which an indicator of energy dissipation is. "The experimental findings confirmed that the wave breaking due to the presence of the structure is a main energy dissipation mechanism which significantly affects wave transmission" [25]. The effectiveness of a breakwater in reducing wave energy can be measured by the amount of wave energy that passes through it. The higher the wave transmission coefficient, the less effective the breakwater is at reducing wave energy. The wave transmission coefficient is a dimensionless number that represents the ratio of the wave energy that is transmitted past a breakwater to the wave energy that would have been transmitted if the breakwater were not present [24]. A wave transmission coefficient of 0 indicates that no wave energy is transmitted past the breakwater, while a wave transmission coefficient of 1 indicates that all the wave energy is transmitted past the breakwater [25].

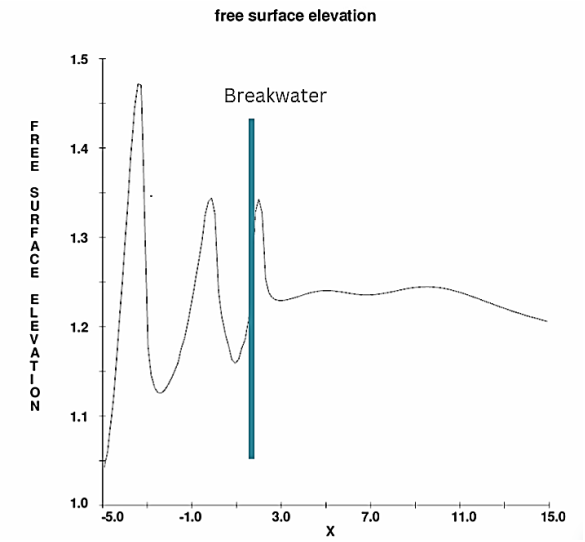

Figure. 7 Graph of wave height throughout the flume

3.2 Wave Transmission and Attenuation

The quantifiable efficiency of the submerged breakwater is summarized by the wave transmission coefficient, K_t, calculated as 0.87. This result indicates that 87% of the incident wave height (H_i)is transmitted past the structure. Consequently, for the specific geometry and wave parameters studied, the decrease of wave height achieved by the breakwater is only 13%, which signifies a moderate level of attenuation.

Calculation of wave transmission:

$$K_t = \frac{H_i}{H_t} \tag{9}$$

$$K_t = \frac{1.2576}{1.4500} \tag{10}$$

$$K_t = 0.87 < 1 \tag{11}$$

$\therefore$ there is energy dissipation

The plot of free surface elevation (Figure. 4) provides the quantitative result of the energy dissipation, showing a sharp, sudden reduction in wave amplitude immediately after the structure's crest at approximately 2.7m. This drop-in wave height is the direct result of the wave-breaking phenomenon and subsequent conversion of energy into turbulence, as qualitatively and quantitatively detailed in the TKE contours in Section 3.1. Post-breakwater, the transmitted wave (H_t) not only exhibits a reduced height but also displays a significantly dispersed profile compared to the initial solitary wave. This noticeable alteration in shape and period (see Figure 4, right side) is critical evidence of the conversion of the coherent, directional kinetic energy of the incident wave into non-directional, internal turbulent energy and frictional heat, which is characteristic of the attenuation process over a submerged structure.

3.3 Quantifying Energy Dissipation

The quantifiable efficiency of the submerged breakwater is summarized by the wave transmission coefficient, K_t, calculated as 0.87 (Equation 9). This result indicates that 87% of the incident wave height (H_i) is transmitted past the structure. Consequently, for the specific geometry and wave parameters studied, the wave height reduction achieved by the breakwater is only 13% ($1 - K_t$), which signifies a significant level of attenuation. Compared to the experimental findings of Grilli et al.,[11] which showed transmission coefficients ranging from 55% to 90% for submerged breakwaters, this paper's result falls on the higher end of this spectrum. This observation suggests that the current design, with a relatively deep submergence head of 0.5m and trapezoidal shape, primarily promotes energy dissipation through wave breaking and turbulence (Section 3.1) rather than through complete reflection or absorption, leading to a higher residual transmitted wave. For this breakwater to meet the design criteria typically associated with effective coastal protection often requiring K_t< 0.7, future optimization of the structural parameters, particularly the submergence depth, is necessary.

The moderate level of attenuation (K_t = 0.87) can be primarily attributed to the design's geometry and submergence condition. With the breakwater crest having a relatively deep head of 0.5 m below the still water level, a substantial portion of the wave energy is permitted to pass over the structure without undergoing the violent energy conversion that occurs during highly confined breaking. Furthermore, the solitary wave used in this simulation may be less conducive to maximum energy transfer than alternative wave forms. This analysis leads to the conclusion that, for the specific geometry and hydrodynamic conditions tested, the breakwater provides sufficient wave height attenuation. Finally, the robustness of the FLOW-3D simulation is supported by the validation results obtained in Section 2, which yielded a correlation

coefficient (R^2) of 0.73 when compared against experimental data. While this coefficient is not unity, it is widely considered an acceptable indicator of accuracy in complex, non-linear free-surface flow modeling using the RNG turbulence closure, aligning with similar standards set in coastal hydrodynamic performance [22]. Therefore, the model is deemed reliable for predicting the wave-structure interaction phenomena and the resulting energy dissipation quantified in this study.

4. CONCLUSIONS

In summary, the primary finding is the quantification of a wave transmission coefficient (K_t) of 0.87, demonstrating that while the 0.5m submerged trapezoidal breakwater effectively induces wave breaking and turbulence (as detailed in the dissipation contour plots in Section 3.1), the overall wave height reduction is moderate compared to literature standards [26][23]. Using FLOW-3D has enhanced the simulation of wave behavior, including breaking waves, compared to traditional CFD methods. FLOW-3D effectively assessed a submerged breakwater's performance in dissipating wave energy. These results suggest submerged breakwaters are a promising solution for coastal protection and can be explored using further refinements of the CFD ranging from different turbulence models that fit coastal demands. This paper is a presentation of a basic model which can be further improved with recent computational capabilities that could benefit coastal structure optimization without using timely procedures like physical modelling which have its own variable limitations. Future real-world validation and field data are recommended to confirm these findings and account for site-specific conditions. Therefore, future research should explore optimizing key design parameters, specifically the submergence depth and crest width, to achieve K_t values closer to the optimal range observed in previous studies, leveraging the validated FLOW-3D model for cost-effective structure optimization.

ACKNOWLEDGEMENTS

This work was conducted as part of the Final Year Project under the Civil Engineering course, assisted by the Civil Engineering Department of the International Islamic University Malaysia. This study was not supported by any grants from funding bodies in the public, private, or not-for-profit sectors.

CONFLICT OF INTEREST

The authors declare no conflicts of interest

AUTHORS' CONTRIBUTION

N.I Khairil Anuar (Writing; Data curation; Formal analysis; Methodology; Validation)

S. Ibrahim (Conceptualization; Formal analysis; Visualisation; Supervision)

I. Ibrahim (Methodology; Data curation; Writing - original draft; Supervision; Resources)

Z. Ramli (Writing - original draft; Resources)

A. T. Hikmatullah Sahib (Writing - review & editing)

A. Abimunya (Formal analysis; Writing - review & editing)

AVAILABILITY OF DATA AND MATERIALS

The data supporting this study's findings are available on request from the corresponding author

ETHICS STATEMENT

Not applicable

REFERENCES

[1] F.A.H. Al-Towayti, H.M. Teh, Z. Ma, I.A. Jae, and A. Syamsir, "Hydrodynamic performance assessment of emerged and sub-merged semicircular breakwaters under random waves: An experimental and empirical study," *PLoS One*, vol. 20, no. 2, p. e0313955, 2025.

[2] R. Afroz, "Experimental and numerical investigation on wave interaction with horizontal slotted submerged porous breakwater," M.S. thesis, Dept. of Water Resources Engineering, Bangladesh University of Engineering and Technology (BUET), Dhaka, Bangladesh, 2015. [Online]. Available: https://www.researchgate.net/publication/278037324-_experimental_and_numerical_investigation_on_wave_interaction_with_horizontal_slotted_submerged_porous_breakwater. Accessed: Nov. 14, 2025.

[3] H.K. Johnson, "Wave modelling in the vicinity of submerged breakwaters," *Coastal Engineering*, vol. 53, no. 1, pp. 39–48, 2006.

[4] C.Y. Li, R.S. Shih, and W.K. Weng, "Visualization investigation of energy dissipation induced by eddy currents for a solitary-like wave passing over submerged breakwater sets," *Journal of Marine Science and Engineering*, vol. 8, no. 11, pp. 1–17, 2020.

[5] P. Wang, K. Fang, G. Wang, Z. Liu, and J. Sun, "Experimental and numerical study of the nonlinear evolution of regular waves over a permeable submerged breakwater," *Journal of Marine Science and Engineering*, vol. 11, no. 8, p. 1610, 2023.

[6] M.A. Islam, M. Bashirul Islam, S. Ul Haque, and O. Abir, "Experimental investigation on the hydrodynamic performance of submerged porous triangular breakwater," *Journal of Engineering Science*, vol. 16, no. 1, pp. 69–80, 2025.

[7] B. Halvorson and Z. Huang, "Study of effects of perforation layouts on wave energy dissipation caused by a submerged perforated breakwater in front of a vertical seawall," *Ocean Engineering*, vol. 311, p. 119025, 2024.

[8] U.A.S.M. Alturfi and A. H. K. Shukur, "Investigation of energy dissipation for different breakwater based on computational fluid dynamic model," *CFD Letters*, vol. 16, no. 1, pp. 22–42, 2024.

[9] X.Y. Wu, X. Liu, Y.K. Chen, and Y. Liu, "Wave energy evolution during Bragg resonance reflection of waves interaction with submerged semicircular breakwaters through the smoothed particle hydrodynamics," *Physics of Fluids*, vol. 37, no. 2, p. 025209, 2025.

[10] Y. Cheng, Z. Lin, G. Hu, and X. Lyu, "Numerical simulation of the hydrodynamic characteristics of the porous I-type composite breakwater," *Journal of Marine Science and Application*, vol. 21, no. 1, pp. 140–150, 2022.

[11] F. Dentale, G. Donnarumma, and E. P. Carratelli, "A new numerical approach to the study of the interaction between wave motion and rubble mound breakwaters," technical paper, MEDUS–University of Salerno/CUGRI, Italy, 2014. [Online]. Available: https://www.flow3d.com/wp-content/uploads/2014/04/A-new-numerical-approach-to-the-study-of-the-interaction-between-wave-motion-and-roubble-mound-breakwaters.pdf

[12] S.T. Grilli, M.A. Losada, and F. Martin, "Characteristics of solitary wave breaking induced by breakwaters," *Journal of Waterway, Port, Coastal, and Ocean Engineering*, vol. 120, no. 1, pp. 74-92, 1994.

[13] K. Kawasaki, "Numerical simulation of breaking and post-breaking wave deformation process around a submerged breakwater," *Coastal Engineering Journal*, vol. 41, no. 3–4, pp. 201-223, 1999.

[14] C.I.N. Izzah, Y. Yunardi, M. Reza, N. Sylvia, N. Malahayati, F. Mulana et al., "Comparative assessment of turbulence models for predicting square cyclone separator performance," *Journal of Advanced Research in Fluid Mechanics and Thermal Sciences*, vol. 127, no. 1, pp. 140–160, 2025.

[15] T. Vermande Paganel, E. Fabrice Alban, M. A. Cyrille, and C. V. Ngayihi Abbe, "CFD simulation of an industrial dust cyclone separator: A comparison with empirical models: The influence of the inlet velocity and the particle size on performance factors in situation of high concentration of particles," *Journal of Engineering*, vol. 2024, no. 1, p. 5590437, 2024.

[16] M.A. Guevara-Luna and L.C. Belalcázar-Cerón, "NGL supersonic separator: Modeling, improvement, and validation and adjustment of k-epsilon RNG modified for swirl flow turbulence model," *Revista Facultad de Ingenieria*, vol. 2017, no. 82, pp. 82–93, 2017.

[17] J. Zhang, Y. Song, Y. Xu, Y. Yang, and J. Wang, "Calibration of RNG k-ε model constants based on experimental data assimilation: A study on the flow characteristics of air-lifted plunger interstitial flow," *Applied Sciences (Switzerland)*, vol. 15, no. 8, p. 4515, 2025.

[18] C.G. Speziale and S. Thangam, "Analysis of an RNG based turbulence model for separated flows," *International Journal of Engineering Science*, vol. 30, no. 10, p. 1379-IN4, 1992.

[19] Y. Tominaga, "Flow around a high-rise building using steady and unsteady RANS CFD: Effect of large-scale fluctuations on the velocity statistics," *Journal of Wind Engineering and Industrial Aerodynamics*, vol. 142, pp. 93–103, 2015.

[20] L. Velásquez, A. Rubio-Clemente, and E. Chica, "Numerical and experimental analysis of vortex profiles in gravitational water vortex hydraulic turbines," *Energies (Basel)*, vol. 17, no. 14, p. 3543, 2024.

[21] E. Kriezi and T. Karambas, "Modelling wave deformation due to submerged breakwaters," *Proceedings of the Institution of Civil Engineers: Maritime Engineering*, vol. 163, no. 1, pp. 19-29, 2010.

[22] D.J. Korteweg and G. de Vries, "On the change of form of long waves advancing in a rectangular canal, and on a new type of long stationary waves," *Philosophical Magazine*, vol. 91, no. 6, pp. 1007–1028, 2011.

[23] N.A. Abd Rahim, K.N. Abdul Maulud, F.A. Mohd, L.H. Lee, and W.H.M. Wan Mohtar, "Evaluation of coastal hydrodynamic performance using statistical analysis at the Kelantan coast, Malaysia," *Malaysian Journal of Society and Space*, vol. 17, no. 4, pp. 393-405, 2021.

[24] J. Shen, H. Wu, and Y. Zhang, "Subsidence estimation of breakwater built on loosely deposited sandy seabed foundation: Elastic model or elasto-plastic model," *International Journal of Naval Architecture and Ocean Engineering*, vol. 9, no. 4, pp. 418-428, 2017.

[25] S.-W. Twu, C.-C. Liu, and W.-H. Hsu, "Wave damping characteristics of deeply submerged breakwaters," *Journal of Waterway, Port, Coastal, and Ocean Engineering*, vol. 127, no. 2, pp. 97-105, 2001.

[26] K.K. Pillai, A. Etemad-Shahidi, and C. Lemckert, "Wave reflection from berm breakwaters," *Proceedings of the Coastal Engineering Conference*, P. Lynett, Ed, no. 36v, no. 7, 2020.